

Supporting Information

Bioadhesion-inspired polymer–inorganic nanohybrid membranes with enhanced CO₂ capture properties

Yifan Li, Shaofei Wang, Hong Wu, Jingtao Wang and Zhongyi Jiang*

1. Experimental

Materials and chemicals: Pebax(R) MH 1657 was purchased from Arkema (French). Dopamine hydrochloride (DA–HCl) was purchased from Wuhan Yuancheng Technology Development Co., Ltd. (China) as dry powder. FeCl₃•6H₂O was purchased from Tianjin Shuangchuan Chemical Reagent Factory. Hydrochloric acid, sodium dodecyl sulphate, ethanol, and n-hexane, were purchased from Tianjin Guangfu Fine Chemical Research Institute (Tianjin, China). All chemicals were of reagent grade or higher, and were used without further purification. Porous PSf hollow fiber membranes were kindly supplied by Tianjin Motian Membrane Engineering and Technology Co., Ltd. (China) with molecular weight cut-off of 6,000.

Preparation of flat sheet homogeneous membranes: A certain amount of Pebax was dissolved in ethanol/water (70/30 wt%) under mild mechanical stirring (with reflux) at 80 °C for 2 h to obtain 3 wt% homogeneous solution. After cooling the solution to ambient temperature, DA–HCl powder was dissolved in it (the weight ratio of DA–HCl to Pebax was 1:10), and the mixed solution was then divided into six aliquots. Different amounts of new-made FeCl₃ aqueous solution (0.33 M) was added into each aliquot, and the Fe³⁺/DA molar ratio (abbreviated as Fe³⁺/DA) was precisely controlled at 0, 1:12, 1:6, 1:3, 1:1.5 and 1:0.75, respectively. As soon as FeCl₃ was added, the solution in each aliquot rapidly turned dark green. After removing bubbles and aging for at least 2 days, the homogeneous solutions were casted onto Teflon plates and then dried under ambient conditions for 24 h, during which the color gradually shifted from green to violet (Fe³⁺/DA=1:12), dark blue (Fe³⁺/DA=1:6,1:3) or black (Fe³⁺/DA=1:1.5,1:0.75), as shown in **Fig. S1**. The membranes were further dried in a vacuum oven at 30 °C overnight to remove the residue solvent. The resultant membranes were designated as Pebax–DA, where iron was absent, or Pebax–Fe(DA)_x, where x means the molar

ratio of DA to iron. For comparison, pure Pebax membrane and Pebax–FeCl₃ membrane were also prepared. It should be mentioned that in the Pebax–FeCl₃ membrane the iron content was equal to that in the Pebax–Fe(DA)₃ membrane. The thickness of all membranes was controlled within the range of 70–90 μm.

Preparation of hollow fiber composite membranes: Hollow fiber composite membranes were prepared through conventional dip-coating methods. Before coating, the PSf hollow fiber substrates were first immersed into ethanol for 48 h, and were further treated with n-hexane for solvent exchange. The solvent remaining at the surface of the hollow fibers was carefully wiped off by filter paper. Then the pre-treated hollow fiber substrates were dipped into the casting solutions for about 15 s, and hung up to dry. After 2 h, another dipping procedure was repeated, and the membranes were hung up up-side-down to let the solvent evaporate. The resultant hollow fiber composite membranes were denoted as X/PSf, where X could be Pebax, Pebax–DA, or Pebax–Fe(DA)_x.

Membrane characterizations: The chemical structure of the Fe³⁺–DA nanoaggregates in membrane was characterized by Raman spectra, which was recorded by a DXR Smart Raman Spectrometer of Thermo Fisher Scientific with Nd:YAG laser (532 nm) as excitation source. The crystalline structures of membranes were determined using wide-angle X-ray diffraction (WAXD) in the range of 10–50° at the speed of 10°/min (Rigaku D/max 2500 v/pc, CuK 40 kV, 200 mA, $\lambda=1.5406\text{ \AA}$). Thermal properties of samples were measured under nitrogen atmosphere by Differential Scanning Calorimetry (DSC) module (PerkinElmer PYRIS Diamond), with the temperature rising from –60 to 250 °C at a heating rate of 10 °C/min. the degree of crystallinity (X_c) of the poly (ethylene oxide) (PEO) segment was calculated through the conventional method.^[S1] Positron annihilation lifetime Spectroscopy (PALS) measurements were performed using an EG&GORTEC fast–fast coincidence system (resolution: 250 ps) at room temperature, with the ²²Na positron source sandwiched by two pieces of 1 mm-thick samples. All the spectra, each with more than a million counts, were recorded and then analyzed in terms of the traditional three-component spectrum using LT-v9 program.^[S2]

Gas permeation experiments: Gas permeation experiments were conducted at 30 °C based on the conventional constant pressure/variable volume technique. The apparatus for testing flat-sheet dense membranes was shown in **Fig. S8**. The pressure of feed gas (pure CO₂ or pure

CH_4) and sweeping gas (N_2) were maintained at 10 bar and 0.1 bar, respectively. The compositions of the feed, retentate, and permeate were measured using Agilent 6820 gas chromatography equipped with a thermal conductive detector (TCD). The permeability (P_i , Barrer, and 1 Barrer = $10^{-10} \text{ cm}^3(\text{STP}) \text{ cm cm}^{-2} \text{ s}^{-1} \text{ cmHg}^{-1}$) of either gas was obtained from the average value of at least twice measurements, by using the equation: $P_i = Q_i l / \Delta p_i A$, where Q_i is the volumetric flow rate of gas ‘*i*’ (cm^3/s) at standard temperature and pressure (STP), Δp_i is the transmembrane pressure difference (cmHg), and A is the effective membrane area, 11.68 cm^2 . The ideal CO_2/CH_4 selectivity (α) was calculated by: $\alpha = P_{\text{CO}_2} / P_{\text{CH}_4}$. To test the gas separation performance of the hollow fiber composite membranes, the prepared fibers were packed into self-made modules, and the effective membrane area of each module was 8.83 cm^2 . Pure gas or mixed gas ($\text{CO}_2/\text{CH}_4 = 20/80 \text{ vol\%}$) measurement was carried out with the feed pressure ranging from 1 bar to 32 bar, by using a device described elsewhere.^[S3] The permeation flux of membrane was characterized by “permeance” ($(P/l)_i$, GPU, and 1 GPU = $10^{-6} \text{ cm}^3(\text{STP}) \text{ cm}^{-2} \text{ s}^{-1} \text{ cmHg}^{-1}$), which was determined by: $(P/l)_i = Q_i / \Delta p_i A$. The ideal or mixed CO_2/CH_4 selectivity (β) was calculated by: $\beta = (P/l)_{\text{CO}_2} / (P/l)_{\text{CH}_4}$.

2. Photographs of the membranes

According to the membrane color, the possible products can be inferred as $[\text{Fe}(\text{L}^{2-})_2]^-$ (violet color), melanochrome (blue color) and melanin (black color),^[S4] of which the oxidation degree of DA becomes deeper sequentially. This could provide additional supports to understand how Fe^{3+} triggers the oxidation and crosslinking reaction of DA.

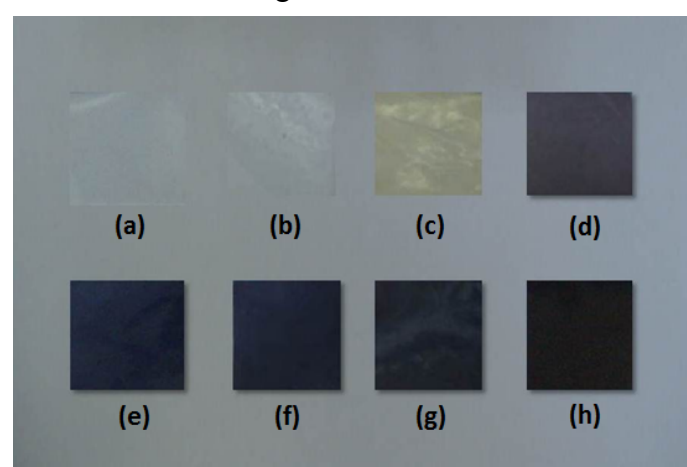


Fig. S1 The photographs of (a) Pebax; (b) Pebax–DA; (c) Pebax– FeCl_3 ; (d) Pebax– $\text{Fe}(\text{DA})_{12}$; (e) Pebax– $\text{Fe}(\text{DA})_6$; (f) Pebax– $\text{Fe}(\text{DA})_3$; (g) Pebax– $\text{Fe}(\text{DA})_{1.5}$; (h) Pebax– $\text{Fe}(\text{DA})_{0.75}$ membranes.

3. TEM of the Fe^{3+} -DA nanoaggregates

TEM images are observed with a Tecnai G2 20 S-TWIN. The morphological images of the *in situ* generated Fe^{3+} -DA nanoaggregates are obtained through dropping the casting solution onto the copper mesh. Few particles can be found when $\text{Fe}^{3+}/\text{DA}=1:12$ (**Fig. S2a**). However, when $\text{Fe}^{3+}/\text{DA}=1:6$, numerous nanoparticles with the diameter of 10–30 nm are observed, indicative of the enhanced cohesive interactions among the Fe^{3+} -DA nanoaggregates. When $\text{Fe}^{3+}/\text{DA}=1:3$, more obvious agglomeration phenomenon is found, confirming the occurrence of further crosslinking of the adhesive particles. In comparison, we observe much larger particles when Fe^{3+} -DA nanoaggregates are generated in polymer-free solvent (Fig. S2d). This implies that the confined space within the polymer matrix restrains the growth of the particles. We further try to retrieve the nanoparticles by high-speed centrifugation (>10000 rpm). To our surprise, the solution remained absolutely clear after centrifugation, implying the density of the particles is close to that of the solvents. These characteristics are beneficial to fabricating thin membranes with homogeneously dispersed nanoparticles.

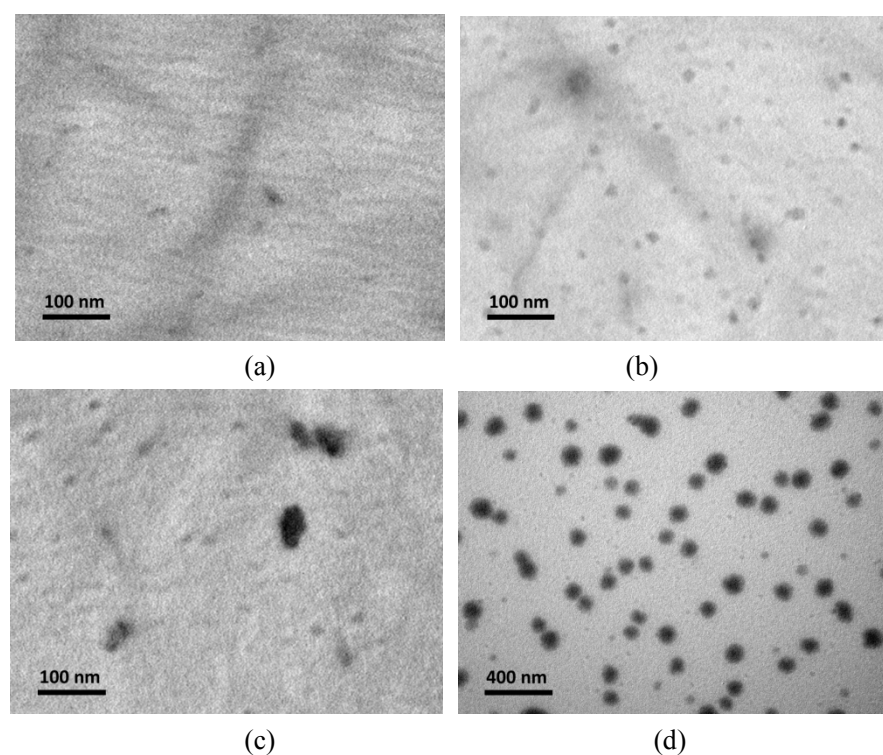


Fig. S2 TEM images of (a)–(c) the *in situ* generated Fe^{3+} -DA nanoaggregates when Fe^{3+}/DA equals to (a) 1:12; (b) 1:6; (c) 1:3; and (d) the Fe^{3+} -DA nanoaggregates generated in the solvent when Fe^{3+}/DA equals to 1:6.

4. DSC curves of the membranes

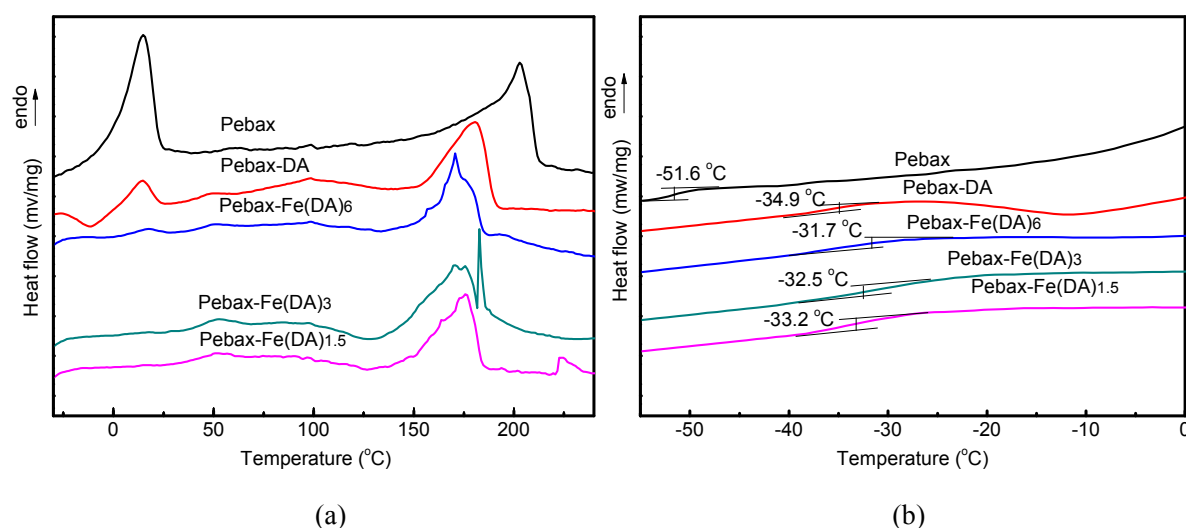


Fig. S3 DSC curves of Pebax, Pebax–DA and Pebax–Fe(DA)_x membranes: (a) high temperature zone; (b) low temperature zone.

5. DMA curves of the membranes

Dynamic mechanical analysis (DMA) curves were obtained with a Q800 DMA instrument (TA Instruments, USA) with a liquid nitrogen cooler. All samples were tested within the temperature range of 203–313 K at a heating rate of 5 K/min, and a frequency of 1Hz was selected for all the experiments.

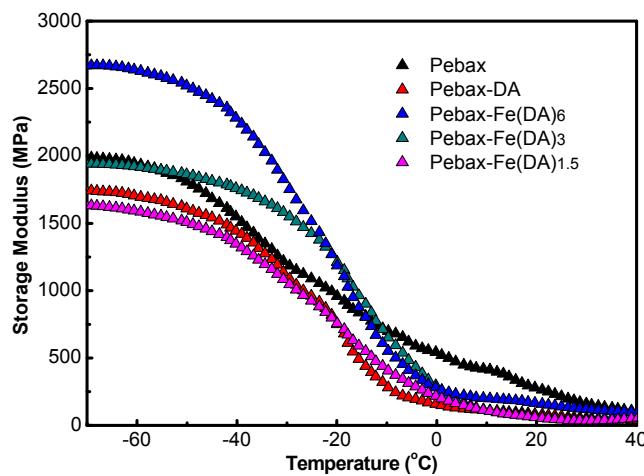


Fig. S4 DMA curves of Pebax, Pebax–DA and Pebax–Fe(DA)_x membranes.

6. Free volume properties of the membranes

In order to acquire more intrinsic structural information that can be directly associated with the diffusion behavior of small molecules in membranes, the free volume properties of membranes were investigated by PALS. On assumption that the location of o-Ps occurs in a sphere potential well surrounded by an electron layer of a constant thickness Δr (0.1656 nm), the radius of free volume cavity (r_3) was calculated from the pick-off annihilation lifetime of o-Ps (τ_3) by the following semi-empirical equation:^[S2]

$$\tau_3 = \frac{1}{2} \left[1 - \frac{r_3}{r_3 + \Delta r} + \left(\frac{1}{2\pi} \right) \sin \left(\frac{2\pi r_3}{r_3 + \Delta r} \right) \right]^{-1}$$

Furthermore, the apparent fractional free volume (FFV) could be estimated by multiplying the volume of equivalent sphere and the intensity of o-Ps (I_3):

$$\text{FFV} = \frac{4}{3} \pi r_3^3 I_3$$

The free volume parameters are listed in **Table 2**.

7. SEM images of the hollow fiber composite membrane

SEM images are observed by using Nanosem 430 field emission scanning electron microscope (FESEM).

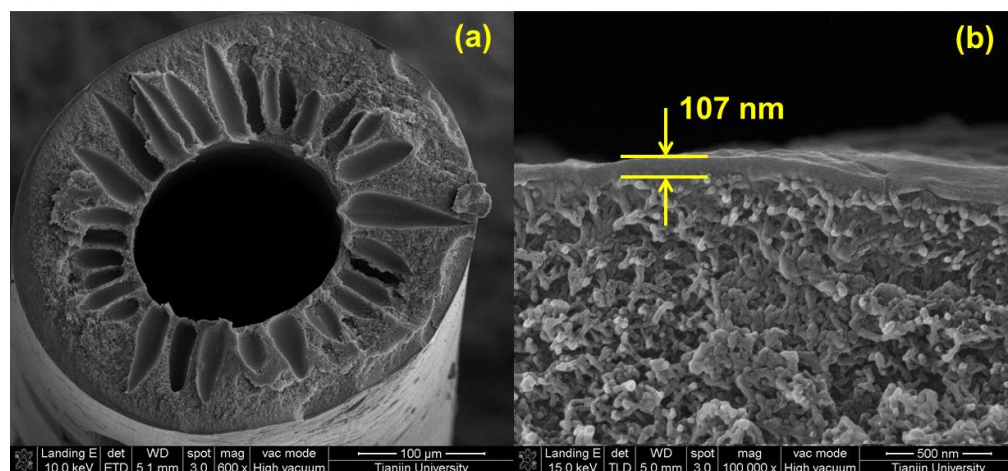


Fig. S5 Cross-section images of Pebax–Fe(DA)₃/PSf hollow fiber composite membrane

8. Gas separation performance of the hollow fiber composite membranes

The results of pure gas test and mixed gas test are plotted in **Fig. S6a** and **S6b**, respectively. The similar trends of the selectivity–permeance curves between dense membrane (**Fig. 4a**) and composite membrane (Fig. S6a) indicate that the effect of PSf substrate is negligible. However, the CO₂ permeance is not as high as the expected value from the permeability of the corresponding dense membrane, which might be partially ascribed to the intrusion of casting solution into the surface pores of PSf substrate, and the resulting denser structure of the transitional zone from the PSf substrate to the skin layer.^[S6] We are currently trying to better understand the relatively high resistance appearing at the interface, and seeking for better substrate structure to obtain higher CO₂ permeance. The comparably lower CO₂ permeance and CO₂/CH₄ selectivity for mixed gas test reveal the existence of coupling effects, resulting from the competing diffusion of CH₄.

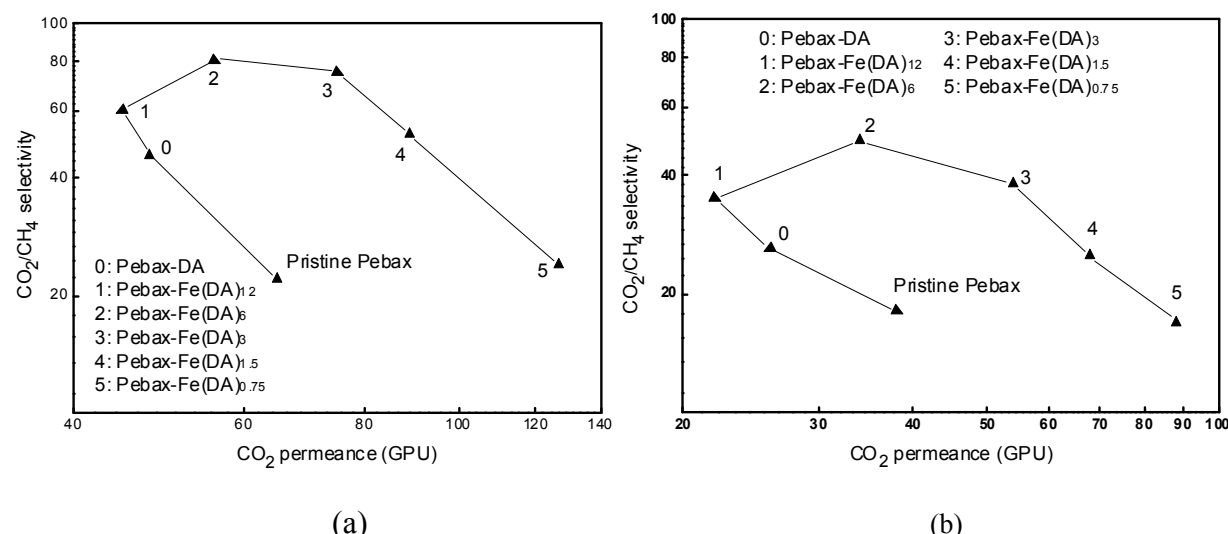


Fig. S6 Relation between CO₂ permeance and CO₂/CH₄ selectivity of Pebax/PSf, Pebax-DA/PSf and Pebax-Fe(DA)_x/PSf composite hollow fiber membranes, tested by using (a) pure CO₂ and pure CH₄; (b) binary CO₂-CH₄ (20/80 vol%) mixed gas at 30 °C and 10 bar.

9. Effect of filler content on membrane performance

The gas separation performance of hybrid membrane usually depends heavily on the filling content of the dispersed species. In this case, Fe(DA)₃ was selected, as the corresponding membrane, Pebax–Fe(DA)₃, outperforms other membranes. While the content of Fe(DA)₃ nanoaggregates increases from 10 wt% to 30 wt%, enhanced CO₂ permeance and lowered CO₂/CH₄ selectivity can be observed (**Fig. S7**), indicative of the loosened membrane structure. Actually, it has been verified by Raman results that Fe³⁺ has been saturated since Fe³⁺/DA reaches 1:3. The most probable reason lies in the lack of active phenol or quinone groups with the progressing of dopamine's polymerization. As such, more content of Fe(DA)₃ may induce lower cohesive force in membrane, which eases the diffusion of CO₂ and CH₄. However, the CO₂/CH₄ selectivity of hybrid membranes maintains higher than that of Pebax control membrane, even if the content of Fe(DA)₃ increases up to 30 wt%. Such interesting results might be explained by the increase of chain stiffness, caused by the rigid structure of Fe(DA)₃ nanoaggregates.

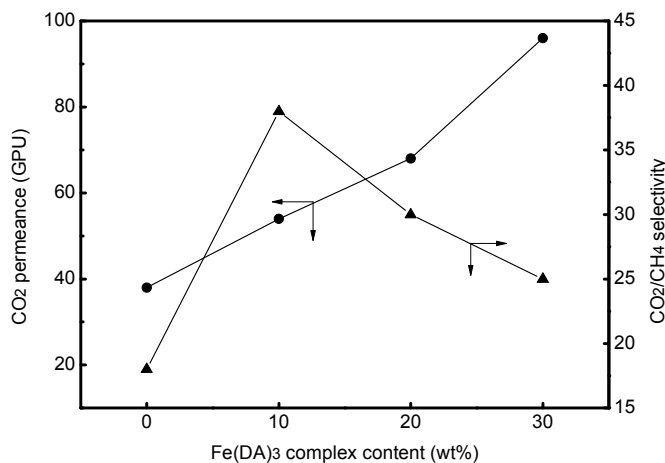


Fig. S7 Effect of Fe(DA)₃ content on membrane performance

10. Pure gas permeation experimental apparatus

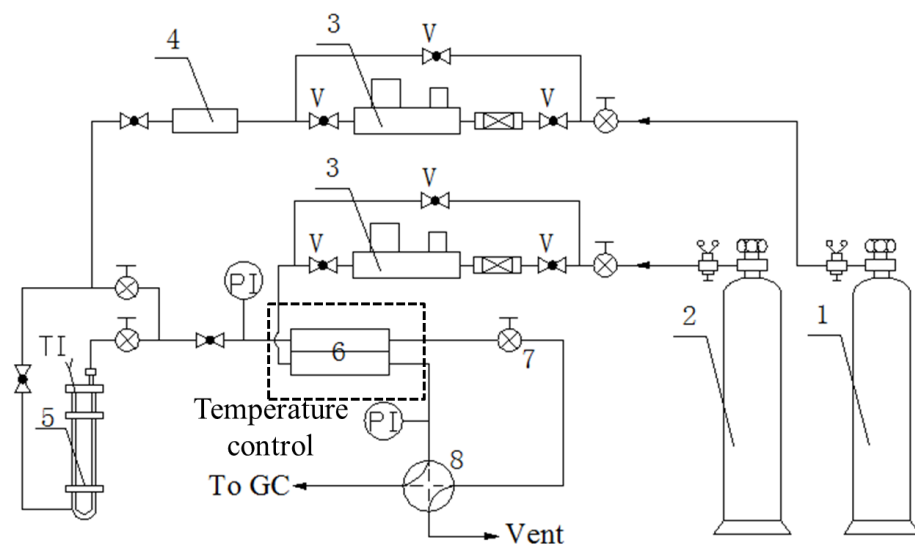


Fig. S8 Pure gas permeation experimental apparatus: (1) feed gas cylinder; (2) sweeping gas cylinder; (3) mass flowmeter; (4) buffer vessel; (5) humidifier; (6) membrane cell; (7) regulating valve; (8) four-way switching valve.

References

- [S1] Y. P. Yampolskii and B. D. Freeman, in *Membrane Gas Separation*, John Wiley & Sons Ltd, Chichester, 2010, pp. 261–265.
- [S2] C. Nagel, K. Günther-Schade, D. Fritsch, T. Strunskus and F. Faupel, *Macromolecules*, 2002, **35**, 2071.
- [S3] F. Pan, H. Jia, S. Qiao, Z. Jiang , J. Wang, B. Wang and Y. Zhong, *J. Membr. Sci.*, 2009, **341**, 279.
- [S4] (a) W. J. Barreto, S. R. G. Barreto and W. P. Silva, *Transit. Metal. Chem.*, 2009, **34**, 677; (b) L. K. Charkoudian and K. J. Franz, *Inorg. Chem.*, 2006, **45**, 3657.
- [S5] F. Peng, L. Lu, H. Sun, Y. Wang, J. Liu and Z. Jiang, *Chem. Mater.*, 2005, **17**, 6790.
- [S6] (a) L. Liu, N. Jiang, C. M. Burns, A. Chakma and X. Feng, *J. Membr. Sci.*, 2009, **338**, 153; (b) S. Tana, L. Li, Z. Zhang and Z. Wang, *Chem. Eng. J.* 2010, **157**, 304.